# Dynamical relaxation behavior of an extended XY chain with a gapless phase following a quantum quench

Kaiyuan Cao and Yayun Hu*
*Zhejiang Lab, Hangzhou 311100, People's Republic of China*

Peiqing Tong†
*Department of Physics and Institute of Theoretical Physics, Nanjing Normal University, Nanjing 210023, People's Republic of China and Jiangsu Key Laboratory for Numerical Simulation of Large Scale Complex Systems, Nanjing Normal University, Nanjing 210023, People's Republic of China*

Guangwen Yang‡
*Zhejiang Lab, Hangzhou 311100, People's Republic of China and Department of Computer Science and Technology, Tsinghua University, Haidian District, Beijing 100084, People's Republic of China*

(Received 12 September 2023; revised 14 December 2023; accepted 18 December 2023; published 9 January 2024)

We investigate the dynamical relaxation behavior of the two-point correlation in extended XY models with a gapless phase after quenches from various initial states. Specifically, we study the XY chain with gapless phase induced by the following additional interactions: Dzyaloshinskii-Moriya interaction and the XZY-YZX type of three-site interaction. When quenching from the gapped phase, we observe that the additional interactions have no effect on the relaxation behavior. The relaxation behavior is $\delta C_{mn}(t) \sim t^{-3/2}$ and $\sim t^{-1/2}$ for the quench to the commensurate phase and the incommensurate phase, respectively. However, when quenching from the gapless phase, we demonstrate that the scaling behavior of $\delta C_{mn}(t)$ is changed to $\sim t^{-1}$ for the quench to the commensurate phase, and the decay of $\delta C_{mn}(t)$ follows $\sim t^{-1}$ or $\sim t^{-1/2}$ for the quench to the incommensurate phase depending on the parameters of pre-quench Hamiltonian. We also establish the dynamical phase diagrams based on the dynamical relaxation behavior of $\delta C_{mn}(t)$ in the extended XY models.

DOI: 10.1103/PhysRevB.109.024303

## I. INTRODUCTION

Advancements in ultracold atomic experiments have sparked significant interest in nonequilibrium many-body physics [1–5]. One particularly important issue of this field is the investigation of the nonequilibrium time evolution of isolated quantum systems over long timescales [6–9]. Numerous studies have focused on the dynamical relaxation of different physical quantities, such as the entanglement entropy [10–14], two-point longitudinal correlation function [15–17], population imbalance [18], antiferromagnetic order parameter [19–21], and ferromagnetic order parameter [22,23]. These studies collectively contribute to a comprehensive understanding of dynamical relaxation in a wide range of physical systems.

Recently, a class of dynamical phase transitions, characterized by the relaxation behavior of the two-point correlation $C_{mn}(t) = \langle\psi(t)|c_m^\dagger c_n|\psi(t)\rangle$, has been proposed in periodically driven systems [10,24–26]. Different from the persistent oscillation behavior [27–29] and the vanishing of the order parameters at critical times of the dynamical quantum phase transitions [30–33], the deviation $\delta C_{mn}(t) = C_{mn}(t) - C_{mn}(\infty)$ of the correlation at time $t$ from their steady-state values decays as a power-law behavior $t^{-\mu}$, where the scaling exponent $\mu$ is determined by the system parameters, suggesting that it characterizes the dynamical phase [10]. Later, this type of power-law scaling behavior has also been observed in the systems following the quantum quench, including the XY model [34] and the XXZ model [35]. Specifically, in the XY chain, two distinct power-law relaxation behaviors have been identified, where the relaxation behavior is $\delta C_{mn}(t) \sim t^{-3/2}$ for the quench to the commensurate phase, and $\delta C_{mn}(t) \sim t^{-1/2}$ for the quench to the incommensurate phase [34]; in the XXZ model [35], the deviation of two-point spin correlation also follows the power-law decay of $t^{-3/2}$. However, a recent article [36] finds that the scaling behavior of $\delta C_{mn}(t)$ may be $\sim t^{-1}$, when the quench is from the critical point (the external field $h_c = 1$) of the Ising transition.

It is well established that additional interactions can lead to different ground-state configurations in the XY chain, which in turn have important implications for various properties. One example is the Dzyaloshinskii-Moriya (DM) interaction, an antisymmetric spin-exchange interaction that plays a crucial role in inducing antiferromagnetic [37–39]. The DM interaction induces the emergence of a gapless phase in the XY

*hyy@zhejianglab.com
†pqtong@njnu.edu.cn
‡ygw@tsinghua.edu.cn

 

chain [40–42]. In this gapless phase, the ground state of the system corresponds to the configuration where all the states with $\varepsilon_k < 0$ are filled and $\varepsilon_k > 0$ are empty. The gapless phase has significant implications for various properties of the quantum system, such as quantum phase transitions [42–45], nonequilibrium thermodynamics [46], dynamical quantum phase transitions [47,48], quantum speed limit [49], and others [50–52]. Therefore, it is highly intriguing to study the impact of the gapless phase on the dynamical relaxation behavior.

In this paper, we study the dynamical relaxation behavior of $C_{mn}(t)$ in the extended XY model with the gapless phase, where the gapless phase is induced by the additional interaction: the DM interaction and the XZY-YZX type of three-site interaction. For a quench from the gapped phase, we find that the dynamical relaxation behavior is not affected by the additional interaction. This is due to the fact that, in both cases, the excitation spectrum satisfies $\varepsilon_k + \varepsilon_{-k} = 2\omega_k$, where $\omega_k$ is exactly the excitation spectrum of the XY chain without the additional interaction. However, for the quench from the gapless phase, we find that the scaling behavior of $\delta C_{mn}(t)$ is changed to $\sim t^{-1}$ for the quench to the commensurate phase, and the decay of $\delta C_{mn}(t)$ follows $\sim t^{-1}$ or $\sim t^{-1/2}$ for the quench to the incommensurate phase depending on the parameters of the prequench Hamiltonian. This change in the scaling behavior can be attributed to the broken inverse symmetry of the excitation spectrum ($\varepsilon_k \neq \varepsilon_{-k}$) induced by the additional interaction. Consequently, the ground state of the prequench Hamiltonian in the gapless phase contains the single-occupied quasiparticle states, which do not contribute to $\delta C_{mn}(t)$.

The paper is organized as follows: In Sec. II, we introduce the general expression of the XY chain with gapless phase and give the formula of $C_{mn}(t)$ for various initial ground states. In Secs. III and IV, we consider the dynamical relaxation behaviors in the XY chain with the DM interaction and the XZY-YZX type of three-site interactions, for which the inverse symmetry of the excitation spectrum is broken. All possible quench protocols are considered. In Sec. V, we discuss the results in the quench from the XX line of the XY model, for which the excitation spectrum satisfies the inverse symmetry with respect to $k = 0$. In Sec. VI, we summarize our results and conclude comments for the dynamical relaxation behavior in the XY chain with the gapless phase.

## II. MODELS

The Hamiltonian for the extended XY chain can be expressed by

$$\begin{aligned} H &= H_{XY} + H_{ex} \\ &= -\frac{1}{2}\sum_{n=1}^{N}\left(\frac{1+\gamma}{2}\sigma_n^x\sigma_{n+1}^x + \frac{1-\gamma}{2}\sigma_n^y\sigma_{n+1}^y + h\sigma_n^z\right) \\ &\quad + H_{ex}, \end{aligned} \tag{1}$$

where $\sigma_n^{x,y,z}$ are the Pauli operators defined on lattice site $n$, $\gamma$ represents the anisotropic parameter, and $h$ denotes the external magnetic field. $H_{ex}$ denotes the additional interaction inducing the gapless phase, given by

$$\begin{aligned} H_{ex} = -\frac{1}{2}\sum_{n=1}^{N}\big[&D\big(\sigma_n^x\sigma_{n+1}^y - \sigma_n^y\sigma_{n+1}^x\big) \\ &+ F\big(\sigma_{n-1}^x\sigma_n^z\sigma_{n+1}^y - \sigma_{n-1}^y\sigma_n^z\sigma_{n+1}^x\big)\big], \end{aligned} \tag{2}$$

where $D$ and $F$ denote the strength of nearest-neighbor and next-nearest-neighbor off-diagonal exchange interaction. When $F = 0$, $H_{ex}$ reduces to the DM interaction, which describes an antisymmetric interaction [37–39,50]. On the other hand, when $D = 0$, $H_{ex}$ describes the next-nearest-neighbor hopping through the XZY-YZX type of three-spin interaction, which introduces gapless phases in the anisotropic XY chain [53–55].

The Hamiltonian can be further expressed as the diagonal form

$$H = \sum_{k>0} H_k = \sum_{k>0}\left[\varepsilon_k\left(\eta_k^\dagger\eta_k - \frac{1}{2}\right) + \varepsilon_{-k}\left(\eta_{-k}^\dagger\eta_{-k} - \frac{1}{2}\right)\right] \tag{3}$$

after using the Bogoliubov transformation $\eta_k = \cos\theta_k c_k + i\sin\theta_k c_{-k}^\dagger$. Here, $\theta_k$ is the Bogoliubov angle. We consider all possible ground-state configurations, in which the ground state is related to the quasiparticle excitation spectrum $\varepsilon_k$, that is [48,56]

$$\begin{aligned} |G\rangle &= \bigotimes_{k>0}|G\rangle_k, \\ |G\rangle_k &= \begin{cases} |0_k0_{-k}\rangle, & \varepsilon_k, \varepsilon_{-k} > 0 \\ |0_k1_{-k}\rangle, & \varepsilon_k > 0, \varepsilon_{-k} \leqslant 0 \\ |1_k0_{-k}\rangle, & \varepsilon_k \leqslant 0, \varepsilon_{-k} > 0 \\ |1_k1_{-k}\rangle, & \varepsilon_k, \varepsilon_{-k} \leqslant 0. \end{cases} \end{aligned} \tag{4}$$

In a quench protocol, the initial state of the system is prepared in the ground state of $H(h_0, \gamma_0)$, i.e., $|\psi_0\rangle = |G\rangle$. At $t > 0$, the Hamiltonian parameters are suddenly changed to $(h_1, \gamma_1)$, and the system is driven by the time-evolution operator $U(t) = e^{-i\tilde{H}t} = e^{-iH(h_1,\gamma_1)t}$. The time-evolved state at the arbitrary time is then given by

$$|\psi(t)\rangle = e^{-i\tilde{H}t}|\psi_0\rangle = \bigotimes_{k>0} e^{-i\tilde{H}_k t}|G\rangle_k, \tag{5}$$

where $|G\rangle_k$ is not the eigenstate of the postquench Hamiltonian $\tilde{H}$.

To observe the dynamical relaxation behavior following the quench, we investigate the fermionic two-point correlation functions $C_{mn}(t) = \langle\psi(t)|c_m^\dagger c_n|\psi(t)\rangle$ following the Refs. [34,36]. By considering the various configurations of the ground states, we obtain the difference $\delta C_{mn}(t)$ of the two-point correlation function from its steady-state values for a long time by

$$\delta C_{mn}(t) = C_{mn}(t) - C_{mn}(\infty) = \int_0^\pi \frac{dk}{2\pi}\delta C_{mn}^k(t), \tag{6}$$

where every component $\delta C^k_{mn}(t)$ is dependent on the initial states, i.e.,

$$\delta C^k_{mn}(t) = \begin{cases} \sin 2\tilde{\theta}_k \sin 2\alpha_k \cos[(\tilde{\varepsilon}_k + \tilde{\varepsilon}_{-k})t] \cos[k(n-m)], & \varepsilon_k, \varepsilon_{-k} > 0 \\ 0, & \varepsilon_k > 0, \varepsilon_{-k} < 0 \\ 0, & \varepsilon_k < 0, \varepsilon_{-k} > 0 \\ -\sin 2\tilde{\theta}_k \sin 2\alpha_k \cos[(\tilde{\varepsilon}_k + \tilde{\varepsilon}_{-k})t] \cos[k(n-m)], & \varepsilon_k, \varepsilon_{-k} < 0. \end{cases} \tag{7}$$

Equation (7) indicates that the single-occupied quasiparticle initial states $|1_k, 0_{-k}\rangle$ and $|0_k, 1_{-k}\rangle$ do not contribute to $\delta C_{mn}(t)$.

## III. EXTENDED XY CHAIN WITH DZYALOSHINSKII-MORIYA INTERACTION

Now we consider the extended XY chain with the DM interaction, in which the Hamiltonian is given by (1) with $F = 0$. By using the Jordan-Wigner and Bogoliubov transformations, the system can be expressed as the diagonal form (3) with the quasiparticle excitation spectrum

$$\varepsilon_k = -2D \sin k + \omega_k, \tag{8}$$

where $\omega_k = [(h + \cos k)^2 + \gamma^2 \sin^2 k]^{1/2}$. The Bogoliubov angles satisfy

$$u_k = \cos\theta_k = \frac{h + \cos k - \omega_k}{\sqrt{2[\omega_k^2 - (h + \cos k)\omega_k]}}, \tag{9}$$

$$v_k = \sin\theta_k = \frac{\gamma \sin k}{\sqrt{2[\omega_k^2 - (h + \cos k)\omega_k]}}. \tag{10}$$

It should be noticed that the Bogoliubov angles are independent of the strength of the DM interaction.

Figure 1(a) displays the phase diagram of the extended XY chain with the DM interaction for $D = 0.2$. The phase diagram consists of four parts: the ferromagnetic phase along the $x$ direction (FM$_x$), the paramagnetic phase (PM), the ferromagnetic phase along the $y$ direction (FM$_y$), and the chiral gapless phase (CP). The dashed line denotes the critical lines between the commensurate and incommensurate phases, corresponding to $h = 1 - \gamma^2$, known as the disorder line (DL). The FM$_x$, FM$_y$, and PM phases are the gapped phases, in which the ground state is

$$|G\rangle = \bigotimes_{k\in(0,\pi]} |0_k 0_{-k}\rangle. \tag{11}$$

The CP phase is the gapless phase, in which the ground state is

$$|G\rangle = \bigotimes_{k_1>0} |0_{k_1} 0_{-k_1}\rangle \bigotimes_{k_2>0} |1_{k_2} 0_{-k_2}\rangle, \tag{12}$$

with $\varepsilon_{k_1} > 0$ and $\varepsilon_{k_2} < 0$.

From Eq. (7), the $\delta C_{mn}(t)$ in the XY chain with DM interaction is given by

$$\delta C_{mn}(t) = \begin{cases} \int_{k\in(0,\pi]} \frac{dk}{2\pi} \delta C^k_{mn}(t), & \text{from the gapped phase} \\ \int_{k\in\{k_1\}} \frac{dk}{2\pi} \delta C^k_{mn}(t), & \text{from the gapless phase,} \end{cases} \tag{13}$$

with

$$\delta C^k_{mn}(t) = \sin 2\tilde{\theta}_k \sin 2\alpha_k \cos(2\tilde{\omega}_k t) \cos[k(m-n)]. \tag{14}$$

It should be noticed that here we have $\tilde{\varepsilon}_k + \tilde{\varepsilon}_{-k} = 2\tilde{\omega}_k$, and $\tilde{\omega}_k$ is exactly the excitation spectrum of the XY chain without the DM interaction.

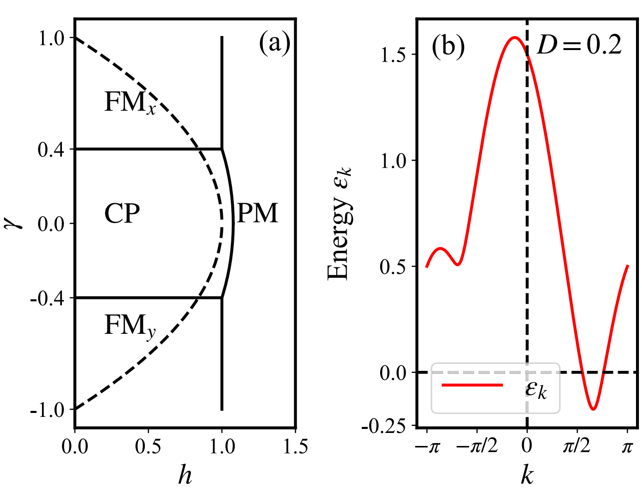


FIG. 1. (a) The phase diagram of the extended XY chain with the DM interaction for $D = 0.2$. The solid line between the CP and PM phases corresponds to $h = (4D^2 - \gamma^2 + 1)^{1/2}$. The dashed line denotes the critical lines between the commensurate and incommensurate phases, corresponding to $h = 1 - \gamma^2$, known as the disorder line. (b) The energy spectra for ($h = 0.5, \gamma = 0.2$) in the CP phase. The energy spectra do not satisfy the inverse symmetry, i.e., $\varepsilon_k \neq \varepsilon_{-k}$.

### A. Quench from gapped phases

First, we consider the quench protocols from the gapped phase. In Fig. 2, we display $\delta C_{mn}(t)$ as a function of $t$ for the quench from the PM phase to both the commensurate and incommensurate phases, where $|n - m| = 1$. It is evident that for the quench from the gapped phase to the commensurate phase, $\delta C_{mn}(t)$ exhibits a scaling behavior of $\sim t^{-3/2}$, while for the quench to the incommensurate phase, the scaling behavior is given by $\delta C_{mn}(t) \sim t^{-1/2}$.

The relaxation behavior of $\delta C_{mn}(t)$ can be explained by the method of stationary-point approximation. For the quench from the gapped phase, we have

$$\delta C_{mn}(t) = \text{Re}[I(t)], \tag{15}$$

where Euler's formula is used to obtain ($|n - m| = 1$)

$$I(t) = \frac{1}{2\pi} \int_0^\pi dk \sin 2\tilde{\theta}_k \sin 2\alpha_k e^{2i\tilde{\omega}_k t} \cos k = \frac{1}{2\pi} \int_0^\pi dk f(k) e^{ig(k)t}, \tag{16}$$

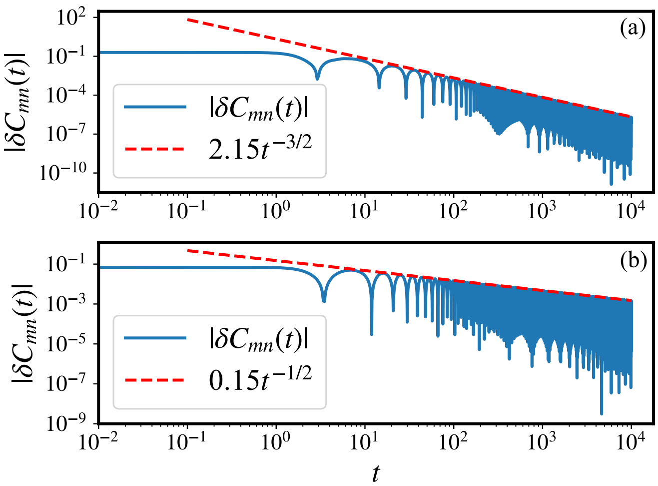


FIG. 2. (a) $|\delta C_{mn}(t)|$ as a function of $t$ for a quench from the PM phase to the commensurate phase, which is from $h_0 = 100$ to $h_1 = 0.9$ with fixed $\gamma_0 = \gamma_1 = 0.5$. (b) $|\delta C_{mn}(t)|$ for a quench from the PM phase to the incommensurate phase, which is from $h_0 = 100$ to $h_1 = 0.5$ with fixed $\gamma_0 = \gamma_1 = 0.2$.

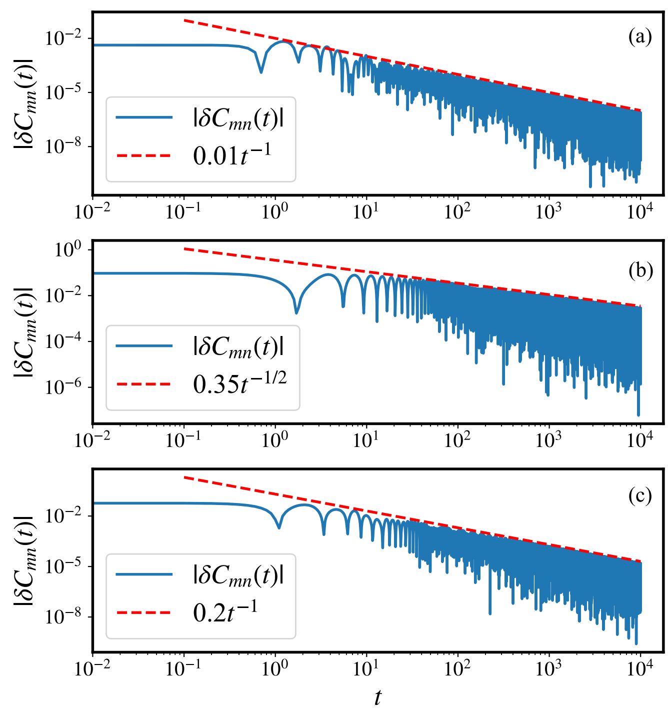


FIG. 3. (a) $|\delta C_{mn}(t)|$ as a function of $t$ for a quench from the CP phase to the commensurate phase, from $h_0 = 0.2$ to $h_1 = 2.0$ with fixed $\gamma_0 = \gamma_1 = 0.2$. $|\delta C_{mn}(t)|$ for a quench from the CP phase to the incommensurate part of FM$_x$ phase, (b) from $(h_0 = 0.2, \gamma_0 = 0.1)$ to $(h_1 = 0.5, \gamma_1 = 0.5)$, and (c) from $(h_0 = 0.2, \gamma_0 = 0.1)$ to $(h_1 = 0.2, \gamma_1 = 0.5)$.

with $f(k) = \sin 2\tilde{\theta}_k \sin 2\alpha_k$ and $g(k) = 2\tilde{\omega}_k$. The exponential term in $I(t)$ oscillates rapidly so that $I(t)$ is determined by the integrals around the stationary points $k_0$, which satisfy $g'(k_0) = 0$. It also should be noticed that, in the XY chain with the DM interaction, the stationary points are given by $\partial\tilde{\omega}_k/\partial k = 0$, which is independent of the DM interaction.

Specifically, for the quench to the commensurate phase, there are two stationary points $k = 0, \pi$. The contributions for the integrals around stationary points $k = 0, \pi$ to $I(t)$ both have the approximate behavior of $\sim t^{-3/2}$ (see Appendix A). Consequently, the relaxation behavior of $\delta C_{mn}(t)$ follows the scaling behavior $t^{-3/2}$ for the long time for the quench from the gapped phase to the commensurate phase. However, for the quench to the incommensurate phase, there is an extra stationary point $k_m$, corresponding to the minimum value of $\tilde{\omega}_k$, besides two stationary points $k = 0, \pi$. The integral around $k_m$ contributes a slower scaling decay $\sim t^{-1/2}$, than that of $k = 0, \pi$. Therefore, the relaxation behavior of $\delta C_{mn}(t)$ dominates for the scaling behavior $\sim t^{-1/2}$, when quenching from the gapped phase to the incommensurate phase.

The dynamical relaxation behavior in the quench protocols from the gapped phase is only determined by whether the postquench Hamiltonian is in the commensurate or incommensurate phase. This is similar to the behavior observed in the XY chain, which suggests that the DM interaction does not affect the relaxation behavior of $\delta C_{mn}(t)$. The reason can be explained by that the excitation spectrum of the XY chain with DM interaction satisfies $\varepsilon_k + \varepsilon_{-k} = 2\omega_k$, where $\omega_k$ is exactly the excitation spectrum of the XY chain.

### B. Quench from gapless phase

Now we consider the quench protocols from the gapless phase. In Fig. 3, we display $\delta C_{mn}(t)$ as a function of $t$ for the quench from the gapless chiral phase to both the commensurate PM phase and incommensurate part of the FM$_x$ phases. It can be observed that, for the quench from the gapless phase to the commensurate PM phase, the scaling behavior is given by $\delta C_{mn}(t) \sim t^{-1}$, and for the quench to the incommensurate phase, the scaling behavior is $\delta C_{mn}(t) \sim t^{-1/2}$ or $\sim t^{-1}$.

To explain the relaxation behavior in the quench protocol from the gapless phase, we can express the function $I(t)$ by

$$I(t) = \frac{1}{2\pi}\left(\int_0^{k_l} + \int_{k_r}^{\pi}\right) dk f(k) e^{ig(k)t}, \tag{17}$$

where $k_l$, $k_r$ are two boundary points, and $\varepsilon_k < 0$ for $k_l < k < k_r$ (see Fig. 4). In this case, the asymptotic behavior of $I(t)$ is determined by the competition between the integrals around stationary points and the boundary points.

Specifically, for the quench from the gapless phase to the commensurate phase, there are two stationary points $k = 0, \pi$ and two boundary points $k_l$, $k_r$ [see Fig. 4(a)]. It is already known that the stationary points $k = 0, \pi$ contribute the scaling decay $\sim t^{-3/2}$. While for the boundary points, according to the generalized Riemann-Lebesgue lemma, the integral around two boundary points in the limited intervals $k \in [0, k_l]$, $[k_r, \pi]$ is given by

$$\sim f(k_l)\frac{e^{2it\tilde{\omega}_{k_l}}}{i\tilde{\omega}'_{k_l}}t^{-1} + f(k_r)\frac{e^{2it\tilde{\omega}_{k_r}}}{i\tilde{\omega}'_{k_r}}t^{-1}. \tag{18}$$

Therefore, the long-time scaling behavior of the integral around the boundary points is $\sim t^{-1}$. As a result, for the quench from the gapless phase to the commensurate phase, the relaxation behavior of $\delta C_{mn}(t)$ follows the slower $\sim t^{-1}$.

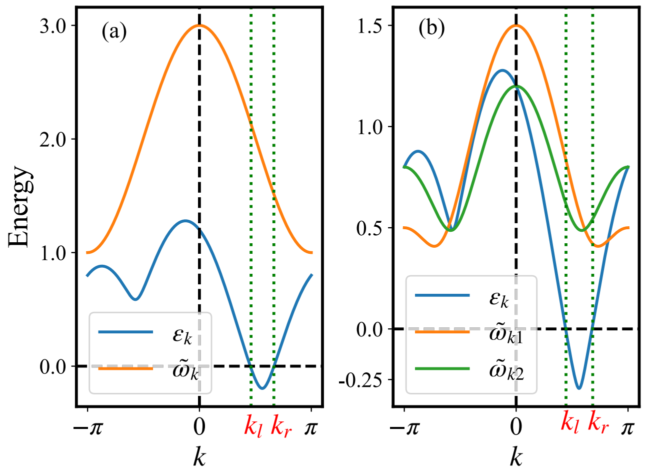


FIG. 4. (a) Energy spectra $\varepsilon_k$ and $\tilde{\omega}_k$ for the prequench Hamiltonian parameter ($h_0 = 0.2, \gamma_0 = 0.2$) and the postquench Hamiltonian parameter ($h_1 = 2.0, \gamma_1 = 0.2$). (b) Energy spectra $\varepsilon_k$, $\tilde{\omega}_{k1}$, and $\tilde{\omega}_{k2}$ for the prequench Hamiltonian parameter ($h_0 = 0.5, \gamma_0 = 0.1$), the postquench Hamiltonian parameters ($h_1 = 0.5, \gamma_1 = 0.5$), and ($h_1 = 0.2, \gamma_1 = 0.5$). The interval $[k_l, k_r]$ does not contain the minimum value of $\tilde{\omega}_{k1}$, but contains the minimum value of $\tilde{\omega}_{k2}$.

While for the quench from the gapless phase to the incommensurate phase, there are two different cases. The first one is that the interval $[k_l, k_r]$ does not contains the minimum points $k_m$ [see the orange line in Fig. 4(b)]. In this case, the asymptotic behavior of $I(t)$ is determined by competition between the integrals around three stationary points $k = 0, \pi, k_m$, and two boundary points $k_l, k_r$. It is evident that the integral around the minimum point $k_m$ contributes the slowest decay $\sim t^{-1/2}$. Consequently, the relaxation behavior of $\delta C_{mn}(t)$ dominates the scaling behavior $\sim t^{-1/2}$ for a long time.

On the other hand, if the interval $[k_l, k_r]$ contains the minimum points $k_m$ [see the orange line in Fig. 4(b)], the stationary point $k_m$ will not contribute to $I(t)$ anymore. In this case, the asymptotic behavior of $I(t)$ is determined by competition between the integrals around two stationary points $k = 0, \pi$, and two boundary points $k_l, k_r$. Similar to the case from the gapless phase to the commensurate phase, the relaxation behavior of $\delta C_{mn}(t)$ follows the scaling behavior $\sim t^{-1}$.

### C. Quench from gapless phase to the disorder line

Now we consider the quench protocol from the gapless phase to the disorder line. The disorder line is the boundary between the commensurate and incommensurate phases in the XY chain. It has already been found a different relaxation behavior of $\delta C_{mn}(t) \sim t^{-3/4}$ for the quench from the gapped phase to the disorder line [34]. In Fig. 5, we display the $\delta C_{mn}(t)$ as a function of $t$ for the quench from the gapless phase to the disordered line. The relaxation behavior of $\delta C_{mn}(t)$ is observed to still follow $\sim t^{-3/4}$. To explain this, we display the excitation spectra $\varepsilon_k$ and $\tilde{\omega}_k$ in the inset graph of Fig. 5. The asymptotic behavior of $\delta C_{mn}(t)$ is determined by the competition between the contributions of stationary points $k = 0, \pi$ and boundary points, in which the contributions of $k = 0$ and two boundary points are $\sim t^{-3/2}$ and $\sim t^{-1}$, respectively. At the stationary point $k = \pi$, we have $d\tilde{\omega}_k/dk|_{k=\pi} = d^2\tilde{\omega}_k/dk^2|_{k=\pi} = 0$, corresponding to the high-order stationary-point approximation. It is known that the high-order stationary point $k = \pi$ contributes the scaling decay for $\sim t^{-3/4}$, which is slower than that for $\sim t^{-3/2}$ and $\sim t^{-1}$. Consequently, the relaxation behavior of $\delta C_{mn}(t)$ follows $t^{-3/4}$ for the quench to the disorder line, regardless of whether the quench originates from the gapped or gapless phase.

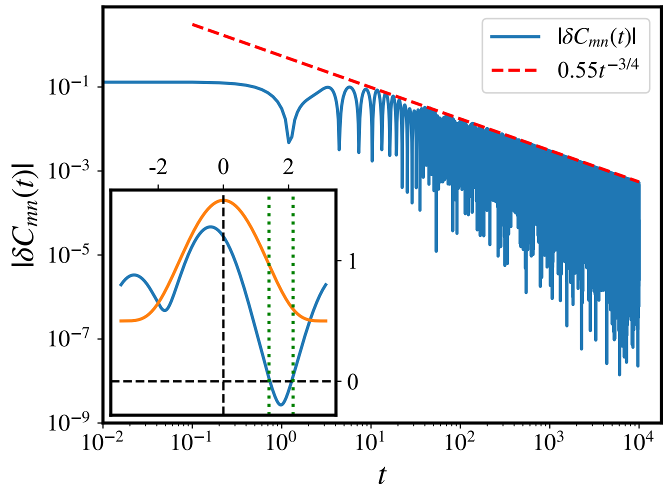


FIG. 5. $|\delta C_{mn}(t)|$ as a function of $t$ for a quench from the gapless chiral phase to the disorder line, which is from ($h_0 = 0.2, \gamma_0 = 0.1$) to ($h_1 = 0.5, \gamma_1 = \frac{1}{\sqrt{2}}$). The inset graph shows energy spectra $\varepsilon_k$ and $\tilde{\omega}_k$ for the Hamiltonian parameters ($h_0 = 0.2, \gamma_0 = 0.1$) and ($h_1 = 0.5, \gamma_1 = \frac{1}{\sqrt{2}}$).

### D. Dynamical phase diagram

In this section, we present a schematic phase diagram that captures the different dynamical phases based on the relaxation behavior of $\delta C_{mn}(t)$. While obtaining the dynamical phase diagram for the quench protocol from the gapped phase is straightforward, as it is divided by the disorder line, we focus on the quench protocol from the gapless phase in this discussion. The dynamical relaxation behavior of $\delta C_{mn}(t)$ is determined by the conditions of whether the postquench Hamiltonian is in the commensurate and incommensurate phases, and whether the interval $[k_l, k_r]$ contains the minimum point $k_m$, as discussed in previous sections. Therefore, the boundary of dynamical phases for the first condition is the disorder line, i.e., $h = 1 - \gamma^2$.

The boundary for the second condition can be obtained by

$$h = \frac{h_0 \pm \sqrt{h_0^2 - \left(1 - \gamma_0^2 + 4D^2\right)\left(h_0^2 + \gamma_0^2 - 4D^2\right)}}{1 - \gamma_0^2 + 4D^2}(1 - \gamma^2), \tag{19}$$

where $h_0$, $\gamma_0$ denote the parameters of the prequench Hamiltonian (see Appendix C). It is important to note that the boundary (19) is dependent on the parameters of the prequench Hamiltonian. The coefficient in (19) represents the solutions of a quadratic equation, resulting in two possible cases for the boundary for $h > 0$. It is known that $1 - \gamma^2 + 4D^2 > 0$ all the times, so that if $h_0^2 + \gamma_0^2 < 4D^2$, we have

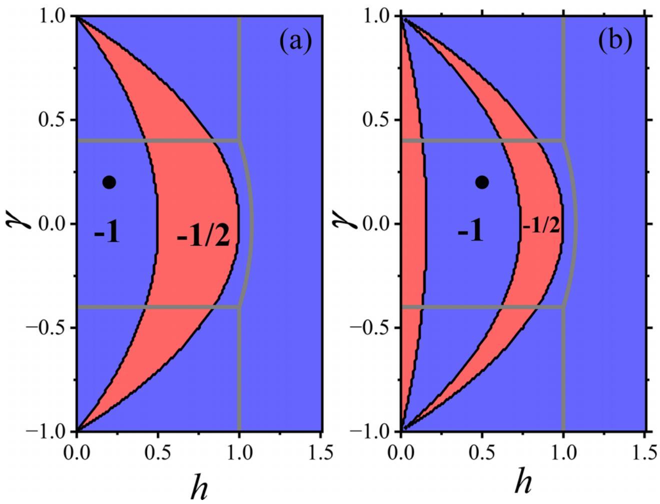

FIG. 6. (a) The dynamical phase diagram for the quench from ($h_0 = 0.2, \gamma_0 = 0.2$) marked by the black solid dot. (b) The dynamical phase diagram for the quench from ($h_0 = 0.5, \gamma_0 = 0.2$). The dynamical phases are characterized by the dynamical relaxation behavior of $\delta C_{mn}(t)$, where the blue region denotes $\delta C_{mn}(t) \sim t^{-1}$, and the red region denotes $\delta C_{mn}(t) \sim t^{-1/2}$. The right boundary is exactly the disorder line.

$h_0 < [h_0^2 - (1-\gamma_0^2+4D^2)(h_0^2+\gamma_0^2-4D^2)]^{1/2}$. In this case, there is one boundary, i.e.,

$$h = \frac{h_0 + \sqrt{h_0^2 - (1-\gamma_0^2+4D^2)(h_0^2+\gamma_0^2-4D^2)}}{1-\gamma_0^2+4D^2}(1-\gamma^2)$$

[see Fig. 6(a)]. If $h_0^2+\gamma_0^2 > 4D^2$, we have $h_0 > [h_0^2 - (1-\gamma_0^2+4D^2)(h_0^2+\gamma_0^2-4D^2)]^{1/2}$. In this case, there two boundaries following Eq. (19) [see Fig. 6(b)].

## IV. RESULTS OF THE XY CHAIN WITH XZY-YZX TYPE OF THREE-SPIN INTERACTION

Now, we consider the XY chain with XZY-YZX type of three-spin interaction, which is described by the Hamiltonian (1) with $D = 0$, $\beta = -1$. Similarly to the XY chain with the DM interaction, the phase diagram consists of four parts see Fig. 7(c): the ferromagnetic phase along the $x$ direction ($FM_x$), the paramagnetic phase (PM), the ferromagnetic phase along the $y$ direction ($FM_y$), and the chiral gapless phase (CP), where, except for the CP phase, $FM_x$, $FM_y$, and PM are the gapped phases. The quasiparticle excitation spectrum is given by [53]

$$\varepsilon_k = \frac{F}{2}\sin 2k + \sqrt{(h+\cos k)^2 + \gamma^2 \sin^2 k}, \quad (20)$$

where the first term $\frac{F}{2}\sin 2k$ breaks the inverse symmetry of the XY chain. Similar to that in the XY chain with the DM interaction, the ground state in the gapped phase ($FM_x$, $FM_y$, and PM phases) is $|G\rangle = \bigotimes_{k>0} |0_k, 0_{-k}\rangle$, and in the gapless phase (CP phase) is $|G\rangle = \bigotimes_{k_1>0} |0_{k_1} 0_{-k_1}\rangle \bigotimes_{k_2>0} |1_{k_2} 0_{-k_2}\rangle$.

It should be noticed that, similar to the case in the XY chain with the DM interaction, the excitation spectrum (20) also satisfies $\varepsilon_k + \varepsilon_{-k} = 2\omega_k$, where $\omega_k$ is the excitation spectrum of the XY chain without the additional interaction. As a

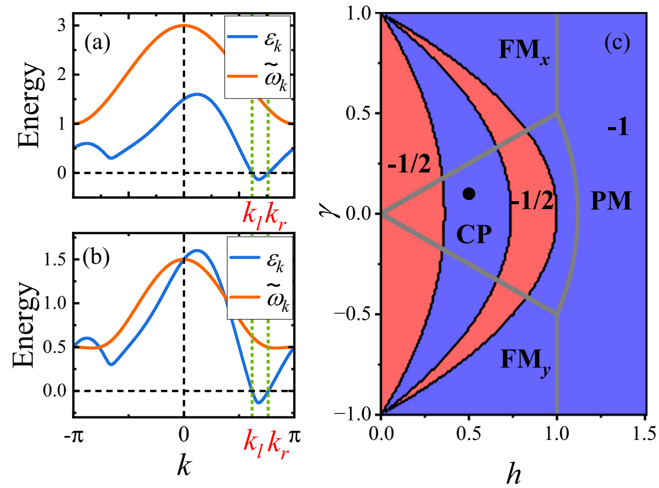

FIG. 7. In the XY chain with XZY-YZX type of three-site interaction, (a) energy spectra $\varepsilon_k$ and $\tilde{\omega}_k$ for the prequench Hamiltonian parameter ($h_0 = 0.5, \gamma_0 = 0.1$) and the postquench Hamiltonian parameter ($h_1 = 2.0, \gamma_0 = 0.5$). (b) $\varepsilon_k$ and $\tilde{\omega}_k$ for the prequench Hamiltonian parameter ($h_0 = 0.5, \gamma_0 = 0.1$) and the postquench Hamiltonian parameter ($h_1 = 0.5, \gamma_0 = 0.65$). (c) The dynamical phase diagram for the quench from ($h_0 = 0.5, \gamma_0 = 0.1$) marked by the black solid dot. The gray solid lines are the critical lines of the quantum phase transitions.

result, for the quench from the gapped phase, the XZY-YZX type of three-site interaction does not influence the relaxation behavior of $\delta C_{mn}(t)$. In the following, we show the results of quenching from the gapless CP phase.

In Fig. 8, we display $|\delta C_{mn}(t)|$ as a function of $t$ for the quench from the gapless chiral phase to both the commensurate PM phase and incommensurate part of the $FM_x$ phases, where $|n-m| = 1$. It can be observed that, for the

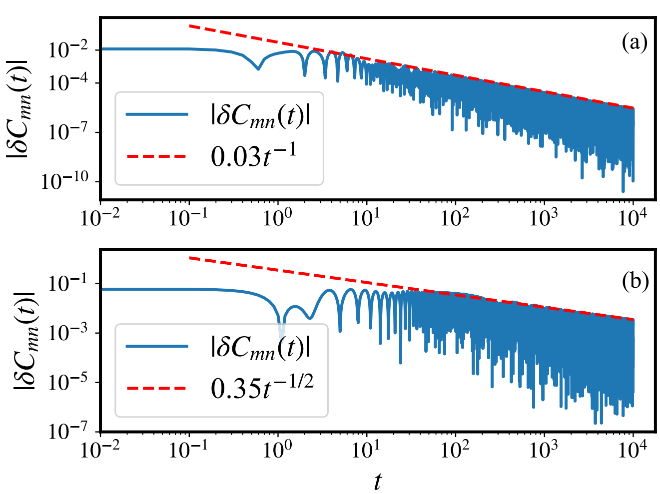

FIG. 8. In the XY chain with XZY-YZX type of three-site interaction, (a) $|\delta C_{mn}(t)|$ as a function of $t$ for a quench from the gapless chiral phase to the commensurate phase, which is from ($h_0 = 0.5, \gamma_0 = 0.1$) to ($h_1 = 2.0, \gamma_1 = 0.5$). (b) $|\delta C_{mn}(t)|$ for a quench from the gapless chiral phase to the incommensurate phase, which is from ($h_0 = 0.5, \gamma_0 = 0.1$) to ($h_1 = 0.5, \gamma_1 = 0.65$).

quench from the gapless phase to the commensurate PM phase, the scaling behavior is given by $\delta C_{mn}(t) \sim t^{-1}$, and for the quench to the incommensurate phase, the scaling behavior is $\delta C_{mn}(t) \sim t^{-1/2}$.

Similarly to the case in the XY chain with the DM interaction, the dynamical relaxation behavior can be explained by the stationary-phase approximation. For the quench from the gapless chiral phase to the commensurate phase, there are two stationary points $k = 0, \pi$ and two boundary points $k_l, k_r$ [see Fig. 7(a)]. As mentioned before, the integrals around the stationary points at the boundary or center of the Brillouin zone provide approximate behavior $\sim t^{-3/2}$, and the boundary points provide $\sim t^{-1}$. Therefore, the power-law behavior of $\delta C_{mn}(t)$ is $\sim t^{-1}$ for the quench from the chiral phase to the commensurate phase. However, for the quench from the gapless chiral phase, the asymptotic behavior depends on whether the interval $(k_l, k_r)$ covers the minimum value of $\tilde{\omega}_k$. As seen in Fig. 7(b), the minimum value of $\tilde{\omega}_k$ is not covered in the interval $(k_l, k_r)$. The integral of $\delta C_{mn}(t)$ is thus contributed by three stationary points $k = 0, \pi, k_m$ ($\tilde{\omega}_{k_m} = \min \tilde{\omega}_k$) and two boundary points $k_l, k_r$, where the integral around $k_m$ provides the slowest asymptotic decay $\sim t^{-1/2}$. Therefore, the power-law behavior of $\delta C_{mn}(t)$ is $\sim t^{-1/2}$, which agrees with the numerical results in Fig. 8(b). If the interval $(k_l, k_r)$ covers the minimum value $\min \tilde{\omega}_k$, the power-law of $\delta C_{mn}(t)$ is $\sim t^{-1}$.

Finally, we obtain the dynamical phase for the quench from the point $(h_0 = 0.5, \gamma_0 = 0.1)$ [see Fig. 7(c)].

## V. RESULTS OF THE QUENCH FROM THE XX LINE

In the previous sections, we discuss the dynamical relaxation behaviors in the XY chain with the DM interaction $(D \neq 0, F = 0)$ and the XZY-YZX type of three-site interaction $(D = 0, F \neq 0)$, respectively. In both models, the energy spectra are asymmetric, so when quenching from the gapless phase, the initial state consists of the vacuum states $|0_k 0_{-k}\rangle$ and the single-occupied state $|1_k 0_{-k}\rangle$. Now, let us consider another special case, i.e., quench from the XX line in the XY chain $(\gamma = 0, D = F = 0, h \leqslant 1)$. In this case, the quasiparticle excitation spectrum $\varepsilon_k$ of the prequench Hamiltonian satisfies the inverse symmetry with respect of $k = 0$, which is given by

$$\varepsilon_k = h + \cos k. \tag{21}$$

To calculate the $\delta C_{mn}(t)$, we consider the XX line as the $\gamma \to 0$ limit.

In Fig. 9, we display the $\delta C_{mn}(t)$ as a function of $t$ for the quench from the gapless chiral phase to both the commensurate PM phase and incommensurate part of the $FM_x$ phases, where $|n - m| = 1$. It can be observed that, for the quench from the gapless phase to the commensurate PM phase, the scaling behavior is given by $\delta C_{mn}(t) \sim t^{-1}$, and for the quench to the incommensurate phase, the scaling behavior is $\delta C_{mn}(t) \sim t^{-1/2}$.

Equation (21) reveals that the quasiparticle excitation spectrum of the XX case satisfies the inverse symmetry with respect to $k = 0$, i.e., $\varepsilon_k = \varepsilon_{-k}$. The inverse symmetry guarantees that the ground state of the prequench Hamiltonian is

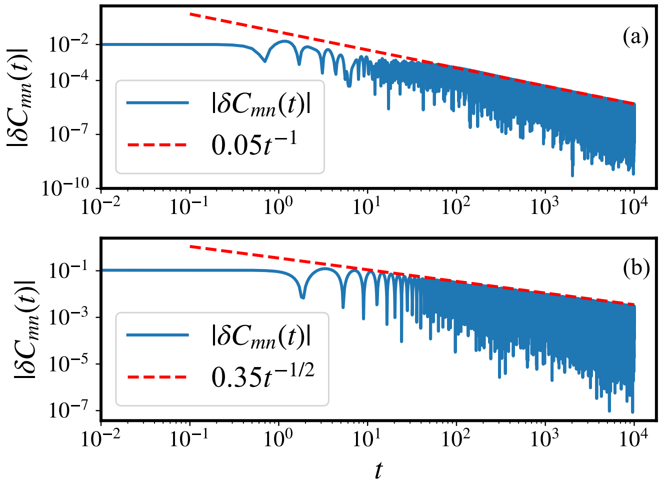


FIG. 9. (a) $|\delta C_{mn}(t)|$ as a function of $t$ for a quench from the XX line to the commensurate phase, which is from $(h_0 = 0.5, \gamma_0 = 0.0001)$ to $(h_1 = 2.0, \gamma_1 = 0.5)$. (b) $|\delta C_{mn}(t)|$ for a quench from the XX line to the incommensurate phase, which is from $(h_0 = 0.5, \gamma_0 = 0.0001)$ to $(h_1 = 0.5, \gamma_1 = 0.5)$.

given by

$$|G\rangle = \bigotimes_{0<k<\kappa} |0_k 0_{-k}\rangle \bigotimes_{\kappa<k<\pi} |1_k 1_{-k}\rangle, \tag{22}$$

with $\varepsilon_k, \varepsilon_{-k} > 0$ for $k < \kappa$ and $\varepsilon_k, \varepsilon_{-k} < 0$ for $k > \kappa$ [see Figs. 10(a) and 10(b)]. The integral of $\delta C_{mn}(t)$ is thus separated as two parts, given by

$$\delta C_{mn}(t) = \frac{1}{2\pi} \int_0^\kappa dk \sin 2\tilde{\theta}_k \sin 2\alpha_k \cos(2\tilde{\omega}_k t) \cos k - \frac{1}{2\pi} \int_\kappa^\pi dk \sin 2\tilde{\theta}_k \sin 2\alpha_k \cos(2\tilde{\omega}_k t) \cos k. \tag{23}$$

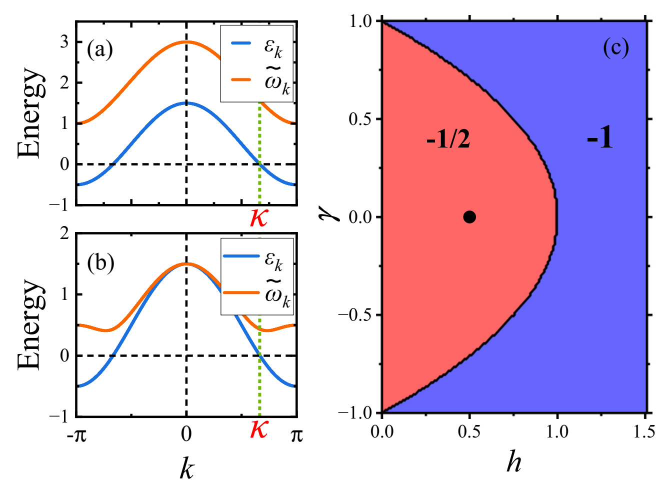


FIG. 10. (a) Energy spectra $\varepsilon_k$ and $\tilde{\omega}_k$ for the prequench Hamiltonian parameter $(h_0 = 0.5, \gamma_0 = 0.0001)$ and the postquench Hamiltonian parameter $(h_1 = 2.0, \gamma_0 = 0.5)$. (b) Energy spectra $\varepsilon_k$ and $\tilde{\omega}_k$ for the prequench Hamiltonian parameter $(h_0 = 0.5, \gamma_0 = 0.0001)$ and the postquench Hamiltonian parameter $(h_1 = 0.5, \gamma_0 = 0.5)$. (c) The dynamical phase diagram for the quench from $(h_0 = 0.5, \gamma_0 = 0.0001)$ marked by the black solid dot.

Therefore, the relaxation behavior of $\delta C_{mn}(t)$ is determined by the integrals around the boundary point $\kappa$ and the stationary points $k = 0, \pi$ and $k = k_m$, where $k_m$ corresponds to the minimum value of $\tilde{\omega}_k$ for the system in the incommensurate phase. It also should be noticed that the case of critical quench in Ref. [36] can be treated as an exceptional case of our theory, in which the zero excitation spectrum $\varepsilon_k = 0$ is located at the center or boundary of the Brillouin zone, i.e., $\kappa = 0, \pi$.

Specifically, for the quench from the XX line to the commensurate phase, the $\delta C_{mn}(t)$ is $\sim at^{-3/2} + bt^{-1}$, which dominates for the scaling behavior of $t^{-1}$ for long time. However, for the quench from the XX line to the incommensurate phase, $\delta C_{mn}(t)$ is $\sim at^{-3/2} + bt^{-1} + ct^{1/2}$, which dominates for the scaling behavior of $\sim t^{-1/2}$. Both of them agree with the numerical results in Fig. 9. According to the relaxation behavior of $\delta C_{mn}(t)$, we plot the dynamical phase diagram as seen in Fig. 10(c). The boundary between the dynamical phases is the disorder line of the commensurate and incommensurate phases.

## VI. CONCLUSION

In this paper, we investigate the dynamical relaxation behavior of extended XY chains with the gapless phase after a quantum quench, in which the gapless phase is induced by the additional interactions: the DM interaction, the XZY-YZX type of three-site interactions, etc. This facilitates us to obtain the expression of the two-point correlation function $C_{mn}(t)$ in the quench from various initial states. We notice that in both models, the excitation spectrum satisfies $\varepsilon_k + \varepsilon_{-k} = 2\omega_k$, where $\omega_k$ is the excitation spectrum of the XY chain without additional interaction. This results in that, when quenching from the gapped phase, the additional interactions do not affect the relaxation behavior. The relaxation behavior is $\delta C_{mn}(t) \sim t^{-3/2}$ for the quench to the commensurate phase, and $\delta C_{mn}(t) \sim t^{-1/2}$ for the quench to the incommensurate phase.

In the case of the quench from the gapless phase, the initial state contains the single-occupied quasiparticle states, i.e., $|1_k 0_{-k}\rangle$, which do not contribute to $\delta C_{mn}(t)$. This indicates that the additional interactions will affect the integral region of $\delta C_{mn}(t)$, and generate the boundary points in the asymptotic behavior. Consequently, we find the dynamical universal decay of the two-point correlation follows a power law of $t^{-1}$ and $t^{-1/2}$, where $t^{-1}$ is contributed by the integral around the boundary point. Specifically, when the quench is from the gapless phase to the commensurate phase, the power-law behavior of $\delta C_{mn}(t)$ is $t^{-1}$. However, when the quench is from the gapless phase to the incommensurate phase, there are two different cases. The one is that the interval $[k_l, k_r]$, in which $\varepsilon_k$ of the prequench Hamiltonian is smaller than zero, covering the minimum value of $\tilde{\omega}_k$ of the postquench Hamiltonian. In this case, the power-law behavior is $t^{-1}$. The other is that the interval $[k_l, k_r]$ does not cover the $\min \tilde{\omega}_k$, where the power-law behavior is $t^{-1/2}$. Finally, we give the dynamical phase diagram and find it also depending on the position of the prequench Hamiltonian.

In addition, we also study the case of quench from the XX line, in which the ground state contains the double-occupied quasiparticle states $|1_k 1_{-k}\rangle$, due to the excitation spectrum satisfying the inverse symmetry with respect to $k = \pi$. The dynamical relaxation behavior of $\delta C_{mn}(t)$ is found to be $\sim t^{-1}$ for the quench from the XX line to the commensurate phase, and $\sim t^{-1/2}$ for the quench from the XX line to the incommensurate phase.

## ACKNOWLEDGMENTS

The work is supported by the National Key Basic Research Program of China (Grant No. 2020YFB0204800), the National Science Foundation of China (Grants No. 12204432, No. 11975126, and No. 12247106), and Key Research Projects of Zhejiang Lab (Grants No. 2021PB0AC01 and No. 2021PB0AC02).

## APPENDIX A: CORRELATION FUNCTIONS

In this paper, we impose the periodic boundary conditions with $\sigma_{N+1} = \sigma_1$. By implementing the Jordan-Wigner transformation, the Hamiltonian (1) can be written as a quadratic form of the spinless fermion model [57]:

$$H = \sum_{mn} c_m^\dagger A_{mn} c_n + \frac{1}{2} \sum_{mn} (c_m^\dagger B_{mn} c_n^\dagger + \text{H.c.}), \tag{A1}$$

where $c_n$ and $c_n^\dagger$ are fermion annihilation and creation operators, respectively. By applying the Fourier transformation, the Hamiltonian is written in momentum space as

$$H = \sum_{k>0} \Psi_k^\dagger \mathbb{H}_k \Psi_k, \tag{A2}$$

where $\Psi_k = (c_k, c_{-k}^\dagger)^T$ are Nambu spinors, and $\mathbb{H}_k$ are the associated Bloch Hamiltonians.

Considering the quasiparticle operators between the pre- and postquench Hamiltonian are related by the Bogoliubov transformation $\eta_k = \cos\alpha_k \tilde{\eta}_k - i \sin\alpha_k \tilde{\eta}_{-k}^\dagger$ with $\alpha_k = \theta_k - \tilde{\theta}_k$, we obtain the eigenstates of the prequench Hamiltonian $H_k$ as a superposition of eigenstates of $\tilde{H}_k$ by

$$\begin{aligned}
|0_k 0_{-k}\rangle &= \cos\alpha_k |\tilde{0}_k \tilde{0}_{-k}\rangle - i \sin\alpha_k |\tilde{1}_k \tilde{1}_{-k}\rangle, \\
|0_k 1_{-k}\rangle &= |\tilde{0}_k \tilde{1}_{-k}\rangle, \\
|1_k 0_{-k}\rangle &= |\tilde{1}_k \tilde{0}_{-k}\rangle, \\
|1_k 1_{-k}\rangle &= -i \sin\alpha_k |\tilde{0}_k \tilde{0}_{-k}\rangle + \cos\alpha_k |\tilde{1}_k \tilde{1}_{-k}\rangle.
\end{aligned} \tag{A3}$$

Then the time-evolved state is given by

$$|\psi_k(t)\rangle = e^{-i\tilde{H}_k t}|G\rangle_k = \begin{cases} \cos\alpha_k e^{i(\tilde{\varepsilon}_k+\tilde{\varepsilon}_{-k})t/2}|\tilde{0}_k\tilde{0}_{-k}\rangle - i\sin\alpha_k e^{-i(\tilde{\varepsilon}_k+\tilde{\varepsilon}_{-k})t/2}|\tilde{1}_k\tilde{1}_{-k}\rangle, & \varepsilon_k, \varepsilon_{-k} > 0 \\ e^{i(\tilde{\varepsilon}_k-\tilde{\varepsilon}_{-k})t/2}|\tilde{0}_k\tilde{1}_{-k}\rangle, & \varepsilon_k > 0, \varepsilon_{-k} \leqslant 0 \\ e^{i(-\tilde{\varepsilon}_k+\tilde{\varepsilon}_{-k})t/2}|\tilde{1}_k\tilde{0}_{-k}\rangle, & \varepsilon_k \leqslant 0, \varepsilon_{-k} > 0 \\ -i\sin\alpha_k e^{i(\tilde{\varepsilon}_k+\tilde{\varepsilon}_{-k})t/2}|\tilde{0}_k\tilde{0}_{-k}\rangle + \cos\alpha_k e^{-i(\tilde{\varepsilon}_k+\tilde{\varepsilon}_{-k})t/2}|\tilde{1}_k\tilde{1}_{-k}\rangle, & \varepsilon_k, \varepsilon_{-k} \leqslant 0. \end{cases} \tag{A4}$$

To obtain $C_{mn}(t)$, we transform the fermionic operators into the momentum space. We obtain

$$C_{mn}(t) = \langle\psi(t)|\frac{1}{N}\sum_k c_k^\dagger c_k e^{ik(n-m)}|\psi(t)\rangle = \frac{1}{N}\sum_{k>0}[\langle\psi_k(t)|c_k^\dagger c_k|\psi_k(t)\rangle e^{ik(n-m)} + \langle\psi_k(t)|c_{-k}^\dagger c_{-k}|\psi_k(t)\rangle e^{-ik(n-m)}], \tag{A5}$$

where

$$\begin{aligned}\langle\psi_k(t)|c_k^\dagger c_k|\psi_k(t)\rangle &= \langle\psi_k(t)|(\cos\tilde{\theta}_k\tilde{\eta}_k^\dagger + i\sin\tilde{\theta}_k\tilde{\eta}_{-k})(\cos\tilde{\theta}_k\tilde{\eta}_k - i\sin\tilde{\theta}_k\tilde{\eta}_{-k}^\dagger)|\psi_k(t)\rangle \\ &= \langle\psi_k(t)|\cos^2\tilde{\theta}_k\tilde{\eta}_k^\dagger\tilde{\eta}_k - i\sin\tilde{\theta}_k\cos\tilde{\theta}_k\tilde{\eta}_k^\dagger\tilde{\eta}_{-k}^\dagger + i\sin\tilde{\theta}_k\cos\tilde{\theta}_k\tilde{\eta}_{-k}\tilde{\eta}_k + \sin^2\tilde{\theta}_k\tilde{\eta}_{-k}\tilde{\eta}_{-k}^\dagger|\psi_k(t)\rangle,\end{aligned} \tag{A6}$$

and

$$\begin{aligned}\langle\psi_k(t)|c_{-k}^\dagger c_{-k}|\psi_k(t)\rangle &= \langle\psi_k(t)|(\cos\tilde{\theta}_k\tilde{\eta}_{-k}^\dagger - i\sin\tilde{\theta}_k\tilde{\eta}_k)(\cos\tilde{\theta}_k\tilde{\eta}_{-k} + i\sin\tilde{\theta}_k\tilde{\eta}_k^\dagger)|\psi_k(t)\rangle \\ &= \langle\psi_k(t)|\cos^2\tilde{\theta}_k\tilde{\eta}_{-k}^\dagger\tilde{\eta}_{-k} + i\sin\tilde{\theta}_k\cos\tilde{\theta}_k\tilde{\eta}_{-k}^\dagger\tilde{\eta}_k^\dagger - i\sin\tilde{\theta}_k\cos\tilde{\theta}_k\tilde{\eta}_k\tilde{\eta}_{-k} + \sin^2\tilde{\theta}_k\tilde{\eta}_k\tilde{\eta}_k^\dagger|\psi_k(t)\rangle.\end{aligned} \tag{A7}$$

To calculate $C_{mn}(t)$, we need to calculate every component in Eqs. (A6) and (A7). According to Eq. (A4), we obtain

$$\langle\psi_k(t)y|\tilde{\eta}_k^\dagger\tilde{\eta}_k|\psi_k(t)\rangle = 1 - \langle\psi_k(t)|\tilde{\eta}_k\tilde{\eta}_k^\dagger|\psi_k(t)\rangle = \begin{cases} \sin^2\alpha_k, & \varepsilon_k, \varepsilon_{-k} > 0 \\ 0, & \varepsilon_k > 0, \varepsilon_{-k} \leqslant 0 \\ 1, & \varepsilon_k \leqslant 0, \varepsilon_{-k} > 0 \\ \cos^2\alpha_k, & \varepsilon_k, \varepsilon_{-k} \leqslant 0, \end{cases} \tag{A8}$$

$$\langle\psi_k(t)|\tilde{\eta}_k^\dagger\tilde{\eta}_{-k}^\dagger|\psi_k(t)\rangle = -\langle\psi_k(t)|\tilde{\eta}_{-k}^\dagger\tilde{\eta}_k^\dagger|\psi_k(t)\rangle = \begin{cases} i\sin\alpha_k\cos\alpha_k e^{it(\tilde{\varepsilon}_k+\tilde{\varepsilon}_{-k})}, & \varepsilon_k, \varepsilon_{-k} > 0 \\ 0, \quad \varepsilon_k > 0, & \varepsilon_{-k} \leqslant 0 \\ 0, \quad \varepsilon_k \leqslant 0, & \varepsilon_{-k} > 0 \\ -i\sin\alpha_k\cos\alpha_k e^{it(\tilde{\varepsilon}_k+\tilde{\varepsilon}_{-k})}, & \varepsilon_k, \varepsilon_{-k} \leqslant 0, \end{cases} \tag{A9}$$

$$\langle\psi_k(t)|\tilde{\eta}_{-k}\tilde{\eta}_k|\psi_k(t)\rangle = -\langle\psi_k(t)|\tilde{\eta}_k\tilde{\eta}_{-k}|\psi_k(t)\rangle = \begin{cases} -i\sin\alpha_k\cos\alpha_k e^{-it(\tilde{\varepsilon}_k+\tilde{\varepsilon}_{-k})}, & \varepsilon_k, \varepsilon_{-k} > 0 \\ 0, \quad \varepsilon_k > 0, & \varepsilon_{-k} \leqslant 0 \\ 0, \quad \varepsilon_k \leqslant 0, & \varepsilon_{-k} > 0 \\ i\sin\alpha_k\cos\alpha_k e^{-it(\tilde{\varepsilon}_k+\tilde{\varepsilon}_{-k})}, & \varepsilon_k, \varepsilon_{-k} \leqslant 0, \end{cases} \tag{A10}$$

$$\langle\psi_k(t)|\tilde{\eta}_{-k}\tilde{\eta}_{-k}^\dagger|\psi_k(t)\rangle = 1 - \langle\psi_k(t)|\tilde{\eta}_{-k}^\dagger\tilde{\eta}_{-k}|\psi_k(t)\rangle = \begin{cases} \cos^2\alpha_k, & \varepsilon_k, \varepsilon_{-k} > 0 \\ 0, & \varepsilon_k > 0, \varepsilon_{-k} \leqslant 0 \\ 1, & \varepsilon_k \leqslant 0, \varepsilon_{-k} > 0 \\ \sin^2\alpha_k, & \varepsilon_k, \varepsilon_{-k} \leqslant 0. \end{cases} \tag{A11}$$

Substituting Eqs. (A8)–(A11) into Eqs. (A6) and (A7), we have

$$\langle\psi_k(t)|c_k^\dagger c_k|\psi_k(t)\rangle = \begin{cases} \cos^2\tilde{\theta}_k\sin^2\alpha_k + \frac{1}{2}\sin 2\tilde{\theta}_k\sin 2\alpha_k\cos[(\tilde{\varepsilon}_k+\tilde{\varepsilon}_{-k})t] + \sin^2\tilde{\theta}_k\cos^2\alpha_k, & \varepsilon_k, \varepsilon_{-k} > 0 \\ 0, & \varepsilon_k > 0, \varepsilon_{-k} \leqslant 0 \\ 1, & \varepsilon_k \leqslant 0, \varepsilon_{-k} > 0 \\ \cos^2\tilde{\theta}_k\cos^2\alpha_k - \frac{1}{2}\sin 2\tilde{\theta}_k\sin 2\alpha_k\cos[(\tilde{\varepsilon}_k+\tilde{\varepsilon}_{-k})t] + \sin^2\tilde{\theta}_k\sin^2\alpha_k, & \varepsilon_k, \varepsilon_{-k} \leqslant 0, \end{cases} \tag{A12}$$

and

$$\langle\psi_k(t)|c_{-k}^\dagger c_{-k}|\psi_k(t)\rangle = \begin{cases} \cos^2\tilde{\theta}_k\sin^2\alpha_k + \frac{1}{2}\sin 2\tilde{\theta}_k\sin 2\alpha_k\cos[(\tilde{\varepsilon}_k+\tilde{\varepsilon}_{-k})t] + \sin^2\tilde{\theta}_k\cos^2\alpha_k, & \varepsilon_k, \varepsilon_{-k} > 0, \\ 0, & \varepsilon_k > 0, \varepsilon_{-k} \leqslant 0 \\ 1, & \varepsilon_k \leqslant 0, \varepsilon_{-k} > 0 \\ \cos^2\tilde{\theta}_k\cos^2\alpha_k - \frac{1}{2}\sin 2\tilde{\theta}_k\sin 2\alpha_k\cos[(\tilde{\varepsilon}_k+\tilde{\varepsilon}_{-k})t] + \sin^2\tilde{\theta}_k\sin^2\alpha_k, & \varepsilon_k, \varepsilon_{-k} \leqslant 0. \end{cases} \tag{A13}$$

These indicate that correlation functions are independent of time for the single-occupied states. For $\varepsilon_k, \varepsilon_{-k} > 0$, we have

$$\begin{aligned}C_{mn}^k(t) &= \langle\psi_k(t)|c_k^\dagger c_k|\psi_k(t)\rangle e^{ik(n-m)} + \langle\psi_k(t)|c_{-k}^\dagger c_{-k}|\psi_k(t)\rangle e^{-ik(n-m)} \\ &= [\langle\psi_k(t)|c_k^\dagger c_k|\psi_k(t)\rangle + \langle\psi_k(t)|c_{-k}^\dagger c_{-k}|\psi_k(t)\rangle]\cos[k(n-m)] \\ &\quad + i[\langle\psi_k(t)|c_k^\dagger c_k|\psi_k(t)\rangle - \langle\psi_k(t)|c_{-k}^\dagger c_{-k}|\psi_k(t)\rangle]\sin[k(n-m)] \\ &= \{1 - \cos 2\tilde{\theta}_k\cos 2\alpha_k + \sin 2\tilde{\theta}_k\sin 2\alpha_k\cos[(\tilde{\varepsilon}_k+\tilde{\varepsilon}_{-k})t]\}\cos[k(n-m)],\end{aligned} \tag{A14}$$

and for $\varepsilon_k, \varepsilon_{-k} \leqslant 0$,

$$C^k_{mn}(t) = \{1 + \cos 2\tilde{\theta}_k \cos 2\alpha_k - \sin 2\tilde{\theta}_k \sin 2\alpha_k \cos[(\tilde{\varepsilon}_k + \tilde{\varepsilon}_{-k})t]\} \cos[k(n-m)]. \tag{A15}$$

$C^k_{mn}(t)$ consists of two components: one is the value of $C^k_{mn}(t)$ in the steady state, i.e.,

$$C^k_{mn}(\infty) = \begin{cases} (1 - \cos 2\tilde{\theta}_k \cos 2\alpha_k)\cos[k(n-m)], & \varepsilon_k, \varepsilon_{-k} > 0 \\ (1 + \cos 2\tilde{\theta}_k \cos 2\alpha_k)\cos[k(n-m)], & \varepsilon_k, \varepsilon_{-k} \leqslant 0, \end{cases} \tag{A16}$$

and the other one is the difference between $C^k_{mn}(t)$ and $C^k_{mn}(\infty)$, i.e.,

$$\delta C^k_{mn}(t) = \begin{cases} \sin 2\tilde{\theta}_k \sin 2\alpha_k \cos[(\tilde{\varepsilon}_k + \tilde{\varepsilon}_{-k})t] \cos[k(n-m)], & \varepsilon_k, \varepsilon_{-k} > 0 \\ -\sin 2\tilde{\theta}_k \sin 2\alpha_k \cos[(\tilde{\varepsilon}_k + \tilde{\varepsilon}_{-k})t] \cos[k(n-m)], & \varepsilon_k, \varepsilon_{-k} \leqslant 0. \end{cases} \tag{A17}$$

## APPENDIX B: STATIONARY-POINT APPROXIMATION FOR THE CASE FROM THE GAPPED PHASE

In the following, we use the stationary-phase approximation to explain the relaxation behavior.

For quenching from the gapped phase to the commensurate phase, there are two stationary points $k_0 = 0, \pi$. By considering the Bogoliubov angles satisfy $\tan 2\theta_k = \gamma \sin k/(h + \cos k)$, we have

$$f(k) = \frac{[h_1\gamma_0 - h_0\gamma_1 + (\gamma_0 - \gamma_1)\cos k]\gamma_1 \sin^2 k}{\omega_k \tilde{\omega}_k^2}, \tag{B1}$$

so that $f(0)$, $f'(0)$, $f(\pi)$, and $f'(\pi)$ vanish. We thus need to expand $f(k)$ around $k_0$ and go to the second-order contribution ($\gamma_0 = \gamma_1$):

$$f(k) = \frac{-(h_1 - h_0)\gamma_1^2}{\omega_{k_0}\tilde{\omega}_{k_0}^2}(k - k_0)^2. \tag{B2}$$

Considering $\omega_0(\tilde{\omega}_0) > \omega_\pi(\tilde{\omega}_\pi)$, the contribution of the stationary point $k_0 = 0$ is quite smaller than that of $k_0 = \pi$. Hence, the approximate behavior of $I(t)$ is determined by the contribution of the stationary point $k_0 = \pi$, i.e.,

$$\begin{aligned} I(t) &\approx \frac{1}{2\pi}\frac{-(h_1 - h_0)\gamma_1^2}{\omega_\pi \tilde{\omega}_\pi^2} e^{2it\tilde{\omega}_\pi} \\ &\quad \times \int_0^{+\infty} dk (k-\pi)^2 e^{it\tilde{\omega}''_\pi (k-\pi)^2} \\ &= \frac{1}{2\pi}\frac{-(h_1 - h_0)\gamma_1^2}{\omega_\pi \tilde{\omega}_\pi^2} e^{2it\tilde{\omega}_\pi + i\phi}\sqrt{\frac{\pi}{\tilde{\omega}''_\pi}} t^{-3/2}. \end{aligned} \tag{B3}$$

The asymptotic behavior of $\delta C_{mn}(t)$ is thus given by

$$\delta C_{mn}(t) = \frac{-(h_1 - h_0)\gamma_1^2}{2\omega_\pi \tilde{\omega}_\pi^2 \sqrt{\pi(\tilde{\omega}''_\pi)^3}} \cos(2\tilde{\omega}_\pi t + \phi) t^{-3/2}. \tag{B4}$$

Here, the cosine terms describes the oscillation of $\delta C_{mn}(t)$, so that the decay of $\delta C_{mn}(t)$ is given by $\sim t^{-3/2}$, which agrees with the numerical simulations in Fig. 2(a).

While for quenching from the gapped phase to the incommensurate phase, there is an additional stationary point of $\tilde{\omega}_{k_m}$ for $0 < k_m < \pi$ besides $k_0 = 0, \pi$, where $\tilde{\omega}_{k_m}$ is the minimum value of $\tilde{\omega}_k$. $I(t)$ should be calculated by summing the integrals over all stationary points, i.e.,

$$I(t) = I_1(t) + I_2(t) + I_3(t), \tag{B5}$$

where $I_1(t), I_2(t) \sim t^{-3/2}$ denotes the integrals around the stationary points $k_0 = 0, \pi$, and

$$\begin{aligned} I_3(t) &\approx \frac{(h_1 - h_0)\gamma_1^2 \sin^2 k_m}{2\pi \omega_{k_m}\tilde{\omega}_{k_m}^2} e^{2i\tilde{\omega}_{k_m}} \int_m^{+\infty} dk e^{it\tilde{\omega}''_{k_m}(k-k_m)^2} \\ &= \frac{(h_1 - h_0)\gamma_1^2 \sin^2 k}{2\omega_{k_m}\tilde{\omega}_{k_m}^2 \sqrt{\pi \tilde{\omega}''_{k_m}}} e^{2it\tilde{\omega}_{k_m} + i\phi} t^{-1/2} \\ &\sim t^{-1/2}, \end{aligned} \tag{B6}$$

denotes the integral around the minimum value of $\tilde{\omega}_k$.

Considering $t^{-3/2}$ decays faster than $t^{-1/2}$, the approximate behavior of $\delta C_{mn}(t)$ is determined by the slowest decay, i.e., $\delta C_{mn}(t) \sim t^{-1/2}$. This result also agrees with the numerical simulations in Fig. 2(b).

## APPENDIX C: BOUNDARY OF THE DYNAMICAL PHASE DIAGRAM

The second condition to distinguish the dynamical phase diagram is whether the interval $[k_l, k_r]$ covers the minimum value of $\tilde{\omega}_k$, which can be expressed by the following equations:

$$\begin{aligned} \varepsilon_k &= 0, \\ \cos k &= \frac{h}{\gamma^2 - 1}. \end{aligned} \tag{C1}$$

Here $\varepsilon_k$ is the excitation spectrum of the prequench Hamiltonian $H(h_0, \gamma_0)$.

For the XY chain with DM interaction, the Eq. (C1) reduces to

$$\begin{aligned} -2D\sin k + \sqrt{(h_0 + \cos k)^2 + \gamma_0^2 \sin^2 k} &= 0, \\ \cos k &= -\frac{h}{1 - \gamma^2}, \end{aligned} \tag{C2}$$

which can be written as a quadratic equation of $h/(1 - \gamma^2)$ by

$$\begin{aligned} &(1 - \gamma_0^2 + 4D^2)\left(\frac{h}{1-\gamma^2}\right)^2 - 2h_0\frac{h}{1-\gamma^2} + h_0^2 + \gamma_0^2 - 4D^2 \\ &= 0. \end{aligned} \tag{C3}$$

The Eq. (C3) can be solved by

$$\frac{h}{1-\gamma^2} = \frac{h_0 \pm \sqrt{h_0^2 - (1-\gamma_0^2+4D^2)(h_0^2+\gamma_0^2-4D^2)}}{1-\gamma_0^2+4D^2}. \tag{C4}$$

Therefore, the boundary of the dynamical phase in the case of quench from the gapless phase is also dependent on the position of the prequench Hamiltonian. A similar conclusion can also be obtained for the XY chain with the XZY-YZX type of three-site interaction.


[1] M. Greiner, O. Mandel, T. W. Hänsch, and I. Bloch, Nature (London) **419**, 51 (2002).
[2] S. Trotzky, Y. A. Chen, A. Flesch, I. P. McCulloch, U. Schollwöck, J. Eisert, and I. Bloch, Nat. Phys. **8**, 325 (2012).
[3] M. Gring, M. Kuhnert, T. Langen, T. Kitagawa, B. Rauer, M. Schreitl, I. Mazets, D. A. Smith, E. Demler, and J. Schmiedmayer, Science **337**, 1318 (2012).
[4] M. Lewenstein, A. Sanpera, and V. Ahufinger, *Ultracold Atoms in Optical Lattices: Simulating Quantum Many-Body Systems* (Oxford University Press, Oxford, 2012).
[5] J. Eisert, M. Friesdorf, and C. Gogolin, Nat. Phys. **11**, 124 (2015).
[6] J. Dziarmaga, Adv. Phys. **59**, 1063 (2010).
[7] A. Polkovnikov, K. Sengupta, A. Silva, and M. Vengalattore, Rev. Mod. Phys. **83**, 863 (2011).
[8] M. Fagotti and F. H. L. Essler, Phys. Rev. B **87**, 245107 (2013).
[9] L. D'Alessio, Y. Kafri, A. Polkovnikov, and M. Rigol, Adv. Phys. **65**, 239 (2016).
[10] A. Sen, S. Nandy, and K. Sengupta, Phys. Rev. B **94**, 214301 (2016).
[11] W.-L. You, J. Phys. A: Math. Theor. **47**, 255301 (2014).
[12] P. Calabrese and J. Cardy, J. Stat. Mech. (2016) 064003.
[13] U. Divakaran, Phys. Rev. E **98**, 032110 (2018).
[14] K. Ohgane, Y. Masaki, and H. Matsueda, Phys. Rev. B **107**, 134201 (2023).
[15] L. Bucciantini, M. Kormos, and P. Calabrese, J. Phys. A: Math. Theor. **47**, 175002 (2014).
[16] C. Babenko, F. Göhmann, K. K. Kozlowski, J. Sirker, and J. Suzuki, Phys. Rev. Lett. **126**, 210602 (2021).
[17] S. Zamani, R. Jafari, and A. Langari, Phys. Rev. B **105**, 094304 (2022).
[18] Z. Cai, C. Hubig, and U. Schollwöck, Phys. Rev. B **96**, 054303 (2017).
[19] P. Barmettler, M. Punk, V. Gritsev, E. Demler, and E. Altman, Phys. Rev. Lett. **102**, 130603 (2009).
[20] P. Barmettler, M. Punk, V. Gritsev, E. Demler, and E. Altman, New J. Phys. **12**, 055017 (2010).
[21] J. Ren, Q. Li, W. Li, Z. Cai, and X. Wang, Phys. Rev. Lett. **124**, 130602 (2020).
[22] M. Elbracht and M. Potthoff, Phys. Rev. B **103**, 024301 (2021).
[23] Z. Cai, Phys. Rev. Lett. **128**, 050601 (2022).
[24] S. Nandy, K. Sengupta, and A. Sen, J. Phys. A: Math. Theor. **51**, 334002 (2018).
[25] M. Sarkar and K. Sengupta, Phys. Rev. B **102**, 235154 (2020).
[26] S. Aditya, S. Samanta, A. Sen, K. Sengupta, and D. Sen, Phys. Rev. B **105**, 104303 (2022).
[27] H. Bernien, S. Schwartz, A. Keesling, H. Levine, A. Omran, H. Pichler, S. Choi, A. S. Zibrov, M. Endres, M. Greiner, V. Vuletić, and M. D. Lukin, Nature (London) **551**, 579 (2017).
[28] O. A. Castro-Alvaredo, M. Lencsés, I. M. Szécsényi, and J. Viti, Phys. Rev. Lett. **124**, 230601 (2020).
[29] G. Delfino and M. Sorba, Nucl. Phys. B **974**, 115643 (2022).
[30] M. Heyl, A. Polkovnikov, and S. Kehrein, Phys. Rev. Lett. **110**, 135704 (2013).
[31] J. C. Budich and M. Heyl, Phys. Rev. B **93**, 085416 (2016).
[32] M. Heyl, Rep. Prog. Phys. **81**, 054001 (2018).
[33] T. Hashizume, I. P. McCulloch, and J. C. Halimeh, Phys. Rev. Res. **4**, 013250 (2022).
[34] A. A. Makki, S. Bandyopadhyay, S. Maity, and A. Dutta, Phys. Rev. B **105**, 054301 (2022).
[35] F. B. Ramos, A. Urichuk, I. Schneider, and J. Sirker, Phys. Rev. B **107**, 075138 (2023).
[36] Y.-T. Zou and C. Ding, Phys. Rev. B **108**, 014303 (2023).
[37] I. Dzyaloshinsky, J. Phys. Chem. Solids **4**, 241 (1958).
[38] T. Moriya, Phys. Rev. **120**, 91 (1960).
[39] J. Perk and H. Capel, Phys. Lett. A **58**, 115 (1976).
[40] R. Jafari, M. Kargarian, A. Langari, and M. Siahatgar, Phys. Rev. B **78**, 214414 (2008).
[41] B.-Q. Liu, B. Shao, J.-G. Li, J. Zou, and L.-A. Wu, Phys. Rev. A **83**, 052112 (2011).
[42] M. Zhong, H. Xu, X.-X. Liu, and P.-Q. Tong, Chin. Phys. B **22**, 090313 (2013).
[43] Z.-A. Liu, T.-C. Yi, J.-H. Sun, Y.-L. Dong, and W.-L. You, Phys. Rev. E **102**, 032127 (2020).
[44] H. Fu, M. Zhong, and P. Tong, Eur. Phys. J. B **93**, 80 (2020).
[45] Y.-G. Liu, L. Xu, and Z. Li, J. Phys.: Condens. Matter **33**, 295401 (2021).
[46] Q. Wang, D. Cao, and H. T. Quan, Phys. Rev. E **98**, 022107 (2018).
[47] H. Cheraghi and S. Mahdavifar, J. Phys.: Condens. Matter **30**, 42LT01 (2018).
[48] K. Cao, M. Zhong, and P. Tong, Chin. Phys. B **31**, 060505 (2022).
[49] Z.-R. Zhu, Q. Wang, B. Shao, J. Zou, and L.-A. Wu, Phys. Rev. A **107**, 042427 (2023).
[50] J. Perk and H. Capel, Physica A (Amsterdam, Neth.) **92**, 163 (1978).
[51] J. H. H. Perk and H. Au-Yang, J. Stat. Phys. **135**, 599 (2009).
[52] Q. Luo, Phys. Rev. B **105**, L060401 (2022).
[53] X. Liu, M. Zhong, H. Xu, and P. Tong, J. Stat. Mech. (2012) P01003.
[54] S. Lei and P. Tong, Physica B (Amsterdam, Neth.) **463**, 1 (2015).
[55] W.-L. You, Y.-C. Qiu, and A. M. Oleś, Phys. Rev. B **93**, 214417 (2016).
[56] M. Zhong and P. Tong, Phys. Rev. E **91**, 032137 (2015).
[57] S. Suzuki, J.-i. Inoue, and B. K. Chakrabarti, Transverse Ising chain (pure system), in *Quantum Ising Phases and Transitions in Transverse Ising Models* (Springer, Berlin, Heidelberg, 2013), pp. 13–46.